Accepted Manuscript

Modulation of the Electrocatalytic Performance of PEDOT-PSS by Reactive Insertion into a Sol-gel Silica Matrix

Halima Djelad, Francisco Huerta, Emilia Morallón, Francisco Montilla

Modulation of the Electrocatalytic Performance of PEDOT-PSS by Reactive Insertion into a Sol-gel Silica Matrix

Halima Djelad[1], Francisco Huerta[2], Emilia Morallón[1], Francisco Montilla[1,*]

[1]Dept. Química Física e Instituto Universitario de Materiales, Universidad de Alicante, Ap. 99, E-03080, Alicante, Spain

[2]Dept. Ingenieria Textil y Papelera, Universitat Politecnica de Valencia, Plaza Ferrandiz y Carbonell, 1. E-03801, Alcoy, Spain

1

Abstract

Poly(3,4-ethylenedioxythiophene) doped with poly-(styrenesulfonate), PEDOT−PSS, films synthesized by electrochemical methods can be considered as poor electrocatalyst for the oxidation of ferrocene in aqueous solution. The rate of electron transfer to that redox probe decays progressively as the amount of deposited polymer increases and the true electroactive area available for the electrochemical reaction shows quite modest figures. We present here an alternative, simple way to enhance the properties of this material which uses, exclusively, electrochemical synthesis methods. The electrocatalytic performance can be significantly improved by inserting the polymer within a pre-deposited, three-dimensional porous silica matrix forming an interpenetrating hybrid material. On the one hand, the modified PEDOT-PSS shows doping levels which trebles the unmodified material. On the other, the electron transfer constant and the true electroactive are for ferrocene oxidation increased by a factor of 2 and 4, respectively.

1. Introduction

Electrode surface modification with accurate control of the building blocks is able to produce integrated molecular systems with extended applications in electroanalysis [1–3]. The use of these modified materials spread out during the last years and, particularly, the sol-gel route offered the opportunity of preparing ceramic-like films under rather mild conditions [4,5]. This soft-chemistry synthesis enhanced the possibility of incorporating temperature sensitive biomolecules, such as enzymes to the silica host layer, resulting in very stable hybrid materials useful for bioanalytical purposes [6].

The surface modification with silica gels is typically performed by coating the electrode with thin films obtained from a sol, which is obtained by the hydrolysis of metal alkoxyde precursors in water/alcohol solutions by conventional techniques such as spin or dip coating or, even, by electro-assisted deposition [7,8]. In this latter method, electrogenerated hydroxide ions trigger the polycondensation of the hydrolysed precursors producing films with very controlled properties, including mesoporous assemblies or compact molecularly imprinted structures, which are useful for the encapsulation of electrocatalytic species [8–11]. Silica is an intrinsic dielectric material whose weak electrochemical properties (electroactivity, electron conductivity) can be enhanced by the incorporation of chemical modifiers such as carbon nanomaterials, metal nanoparticles or conducting polymers giving rise to the so-called hybrid silica materials [12,13]. Particularly, conducting polymers are very interesting components for several applications because of their tuneable properties. For example, polyaniline can be grown through porous sol–gel silica films by electrochemical reactive insertion. Silica favours the fast growth of polymer due to confinement effects of oligomeric species formed upon oxidation [14]. These silica–PANI hybrids show enhanced

electrochemical capacitance, since silica matrix avoids the electric collapse between vicinal conducting fibres but allow the diffusion of ionic species in contact with the conjugated polymer [7]. The modulated permselectivity of silica for electroactive species turns into an ability to discern between positively and negatively charged species and, accordingly, this material can be used as preconcentration agent in electrochemical sensing [15]. The improved electrochemical properties of silica-conducting polymer hybrids were used to develop electrodes for direct electrochemistry of cytochrome c, cyt c, encapsulated within a silica film. The electrochemical insertion of poly(3,4-ethylenedioxythiophene) doped with poly-(styrenesulfonate), PEDOT−PSS, through the silica pores connects electrically protein molecules, giving rise to a 3-fold enhancement in the cyt c electrochemical reduction rate [11]. This material has been also employed in sensor devices because of its outstanding properties. For example, organic PEDOT-based electrochemical transistors were used for the simultaneous detection of glucose and lactate [16] and voltammetric sensors based on the same material were used to determine neurotransmitters [17] glucose [18] or cytochrome c [19] in aqueous medium.

PEDOT-PSS is commercially available in the form of suspensions for a straightforward surface modification. However, it can be deposited on suitable electrodes by electrochemical polymerization for a better control of the film properties (morphology, thickness, etc.). Since the solubility in water of EDOT monomer is rather low, the addition of a surfactant is usually required. We will make use of PSS, which acting also as a polyelectrolyte, provides sufficient ionic conductivity to the aqueous solution. After electrochemical deposition, PSS remains within the structure of polymeric PEDOT as the doping agent [20].

PEDOT can be applied as the transducer element of biosensors where oxygen-containing species, such as peroxides, can act as mediators for the charge transfer from redox enzymes [21,22]. Additionally, this polymer has been used to develop second-generation biosensors that incorporate redox species as mediators (quinones, ruthenium complexes, ferrocene, ferricyanide, etc.) to perform the electron transfer.

Among the available redox mediators, ferrocene derivatives received special attention. Ferrocene is commonly classified as an outer-sphere redox probe, which is considered to lack any adsorption step and to show low reorganization energies upon redox transitions [23]. For those reasons, ferrocene has been used routinely to investigate electron-transfer kinetics in chemically modified electrodes [24,25]. Besides, ferrocene has been employed in the development of efficient biosensors [26,27] and also to induce electron transfer from PEDOT films to glucose oxidase or horseradish peroxidase, among other enzymes [28,29].

The present work focuses on the electrochemical synthesis of modified electrodes containing PEDOT-PSS films and their application to the study of ferrocene redox reactions. In this way, the electrocatalytic performance of PEDOT-PSS modified electrodes will be tuned by inserting this conducting polymer within electrodeposited silica matrices and, afterwards, the electrochemical performance of the hybrid material will be explored for ferrocene redox processes. All the electrode modifications will be performed, exclusively, by electrochemical methods.

2. Experimental part

Reagents used in this work were tetraethyl orthosilicate (TEOS, Sigma-Aldrich, reagent grade), ethanol (EtOH) (Sigma-Aldrich, p.a.), potassium chloride (Merck, p.a.),

hydrochloric acid (Merck, reagent grade), sulfuric acid (Merck, p.a.), 3,4-ethylendioxythiophene (EDOT) (Sigma-Aldrich 97%), poly(sodium 4-styrenesulfonate) (PSS) (Sigma-Aldrich p.a.) and ferrocene (Sigma-Aldrich, p.a.).

All solutions were prepared with purified water obtained from an ELGA Lab Water Purelab system (18.2 MΩ cm). Electrochemical experiments were performed in conventional electrochemical glass cells. The working electrode was a glassy carbon rod (GC, geometric area = 0.07 cm^2, Carbone Lorraine, model V-25). The current densities expressed are referred to that geometric area. The GC electrode was carefully polished with emery paper and subsequently rinsed with ultrapure water. A platinum wire was employed as counter electrode, and a reversible hydrogen electrode introduced in the same electrolyte solution placed in Luggin capillary was used as reference electrode. Electrochemical experiments were performed with an eDAQ Potentiostat (EA163 model) coupled to a EG&G Parc Model 175 wave generator and the data acquisition was performed with a eDAQ e-corder 410 unit (Chart and Scope Software).

EDOT electropolymerization was carried out in aqueous medium prepared by dissolving 1.46 g PSS in 10.0 mL ultrapure water, 53 μL EDOT monomer were then added and the resulting solution was stirred in an ultrasonic bath for 30 minutes.

The precursor solution to synthesize silica was 6 mL of TEOS (0.0269 mol), 8.2 mL of EtOH and 5.8 mL of a solution 0.01M HCl + 0.46 M KCl (this salt was added to provide conductivity to the solution). This mixture was stirred for one hour in a close vial. The silica was obtained by electrochemical methods on glassy carbon (GC) rods. The electrode was immersed in that solution and connected to the negative terminal of a power source. A constant current of –2.5 mA cm^{-2} was applied to trigger the reduction of water and an increase in the pH near the electrode, causing the transition of silica to

gel. This current was applied for 1 minute. A Pt wire was used as the anode in this set-up. After silica deposition on GC, the electrode was rinsed with ultrapure water and kept humid (in hydrogel state).

The surface morphology of modified glassy carbon electrodes was studied by field-effect scanning electron microscopy (FESEM, ZEISS model Merlin VP Compact). X-ray photoelectron spectroscopy (XPS, K-ALPHA, Thermo Scientific) was used to analyse the surface composition. All spectra were collected using Al K radiation (1486.6 eV), monochromatized by a twin crystal monochromator, yielding a focused X-ray spot (elliptical in shape with a major axis length of 400 μm) at 3 mA × 12 kV. The alpha hemispherical analyser was operated in the constant energy mode with survey scan pass energies of 200 eV to measure the whole energy band and 50 eV in a narrow scan to selectively measure individual elements. XPS data were analysed with Avantage software. A smart background function was used to approximate the experimental backgrounds, and surface elemental compositions were calculated from background-subtracted peak areas. Charge compensation was achieved with the system flood gun that provides low-energy electrons and low-energy argon ions from a single source. The experimental curves were adjusted using a combination of Lorentz (30%) and Gaussian (70%) functions.

3. Results and discussion

3.1. Electrochemical synthesis of PEDOT-PSS films

Figure 1 shows cyclic voltammograms recorded for a glassy carbon (GC) electrode in the course of EDOT monomer oxidation in aqueous solution containing PSS as the electrolyte.
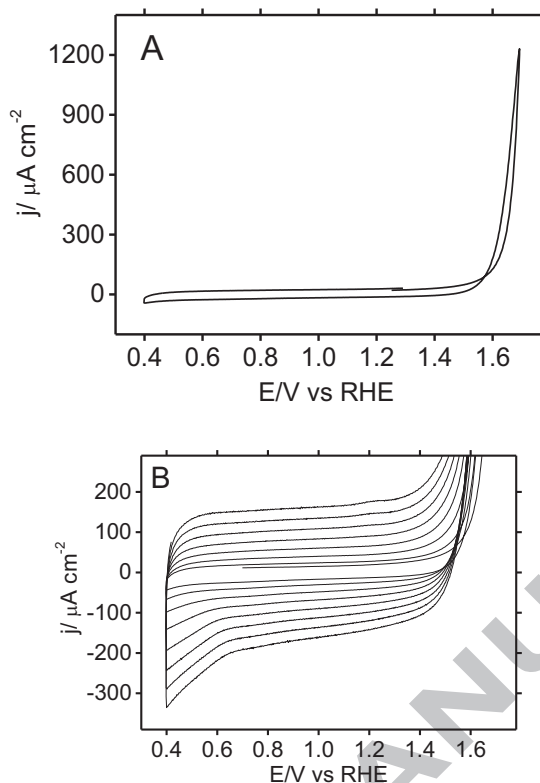
Figure 1: (A) First cyclic voltammogram **(B)** Successive cyclic voltammograms

obtained for a GC electrode in EDOT aqueous solution containing PSS. Scan rate 50

mVs^{-1}

During the first forward scan, the current density is almost zero within the potential region comprised between 0.4 and 1.5V. The monomer oxidation starts at around 1.6V and proceeds with fast electrochemical kinetics, as deduced from the high slope of the *j-E* curve. In successive potential cycles, the progress of a current plateau between 0.4V and 1.5V reveals the capacitance-like response of the deposited PEDOT-PSS film, while the polymer mass can be readily determined at any time from its double-layer charge, assuming a value of 70 F g^{-1} for the specific capacitance [11,30]. The surface morphology of deposited PEDOT-PSS films was examined with the aid of

a field emission SEM device. Figure 2 shows micrographs obtained for different electrodes with increasing mass of deposited polymer ranging between 46.5 and 815 μg cm^{-2}. All films cover uniformly the whole surface of the GC substrates, although they can be observed more clearly when larger amounts of polymeric material are deposited (Figures 2B to 2D). Some crack-like defects, particularly those appearing in Figures 2C and 2D, are generated by the drying process. It is worth mentioning that the surface homogeneity of these PEDOT-PSS films contrasts with some literature data. For example, it was reported either a granular aspect when the material is deposited from organic solvents [31] or an aggregated, cauliflower-like, structure when it was deposited from aqueous solutions on gold substrates [32]. The favourable interaction between carbon support and polymer layer seems at the origin of the smoother morphology shown by our samples.
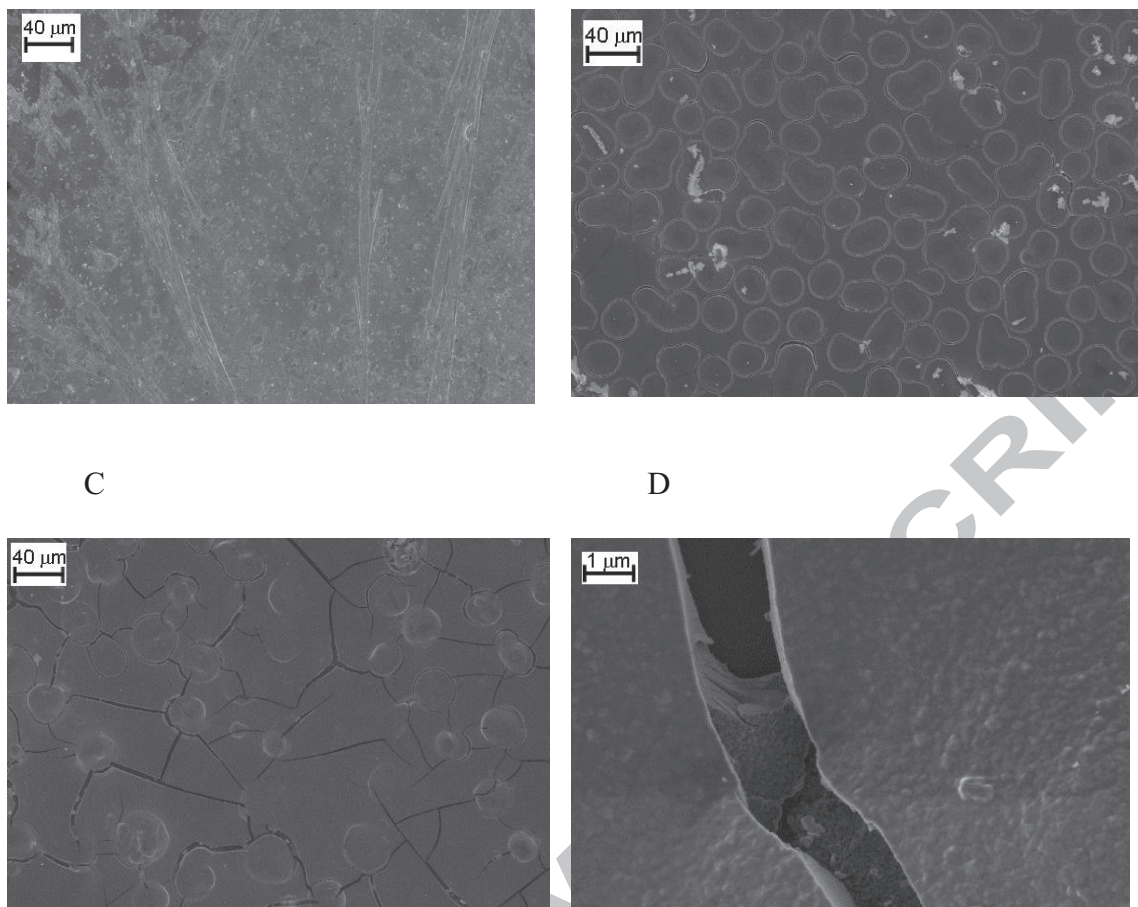
A   B

C   D

Figure 2: FESEM images of PEDOT-PSS films deposited on GC electrodes. Mass of polymer: A) 46.5 μg cm^{-2}; B) 202 μg cm^{-2}; C) and D) 815 μg cm^{-2}

High resolution X-ray photoelectron spectroscopy (XPS) has been employed to characterize the chemical structure of PEDOT-PSS coatings. A glassy carbon electrode covered with a mass of deposited polymer close to 202 μg cm^{-2} (as in Figure 2B) was transferred to the UHV chamber, where C, O and S spectral regions were analysed. The recorded C 1s core level spectrum is depicted in Figure 3A, where three main contributions at 284.5, 285.5 and 286.8 eV can be clearly distinguished. The peak at lower binding energy corresponds to carbon located either in the aromatic backbone of

PEDOT or at the phenyl moieties of PSS. Besides, the contribution at 285.5 eV is originated from C atoms directly bound to S atoms, as those present in both EDOT and PSS units. Finally, the high energy element at 286.8 eV can be assigned to C-O-C structures present at EDOT moieties [33–35].
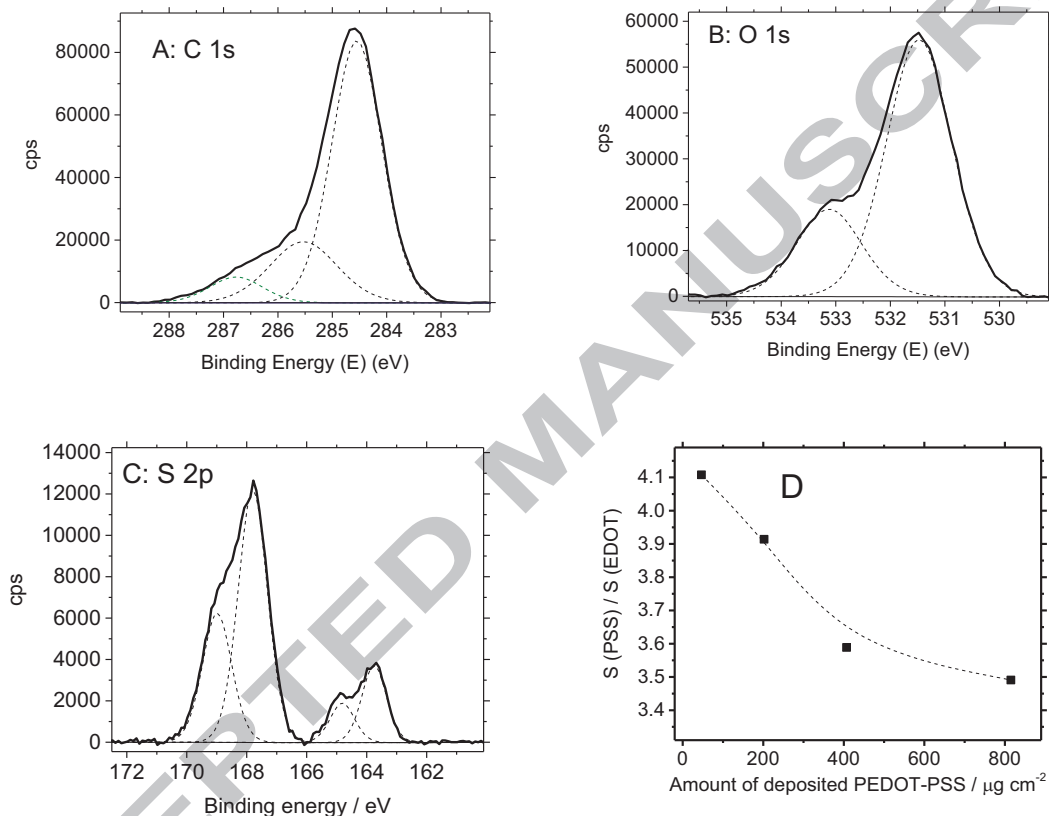

Figure 3: High resolution XPS spectra acquired for: (A) C1s region; (B) O 1s region and (C) S 2p region of a PEDOT-PSS film (202 μg cm^{-2}) deposited on GC. (D) Sulfonate-to-EDOT ratio obtained from the S 2p$_{3/2}$ signals for electrodes covered with different amounts of deposited PEDOT-PSS.

Regarding the O 1s signal (Figure 3B), it can be deconvoluted into two major contributions at 531.5 and 533.1 eV. The peak at lower binding energy is consistent with the presence of PSS sulfonate groups [34], whereas the 533.1 eV peak relates to those oxygen atoms present at the dioxyethylene bridge in EDOT units and also to a high binding energy contribution of PSS [36].

Finally, the S 2p region of the photoelectronic spectrum is shown in Figure 3C. It is characterized by the presence of two major bands corresponding to sulphur species with different oxidation states. Both signals can be deconvoluted into two contributions, showing a characteristic separation between the $2p_{3/2}$ and $2p_{1/2}$ spin-split doublets of 1.18 eV. The low-energy signal, with an S $2p_{3/2}$ contribution at 163.8 eV, is assigned to sulphur atoms located at the thiophene rings in EDOT monomers. Besides, the S $2p_{3/2}$ contribution to the higher binding energy signal (167.9 eV) is attributed to sulphur in a higher oxidation state, which corresponds to those sulfonate groups contained in the PSS dopant anion [34,36,37].

From the ratio of both S 2p signals, the sulfonate to thiophene proportion in any sample of electrodeposited polymer can be conveniently obtained. Such a proportion was calculated for a number of samples and plotted against the amount of deposited polymer in Figure 3D. The plot suggests an excess of PSS dopant content for extremely thin samples (up to 4.1 S atomic ratio) and the occurrence of a progressive depletion of polyelectrolyte ions for films with higher amount of deposited polymer.

3.2. Electrochemical behaviour of ferrocene at unmodified PEDOT-PSS films

We will examine first the electrocatalytic performance of pristine PEDOT-PSS films toward a typical redox mediator as ferrocene. For comparative purposes, the

electrochemical activity of a bare glassy carbon electrode has also been included in the study (Figure 4A). The electrochemical oxidation of the ferrocene redox centre, $Fe^{2+} \rightarrow Fe^{3+}$, at GC substrates is characterized by the presence of a reversible anodic peak centred at 0.515 V in acidic medium. The faradic counter-process occurs at 0.385 V during the reverse scan. As a result, the peak separation between anodic and cathodic features, ΔE_P, is 130 mV under the experimental conditions employed.
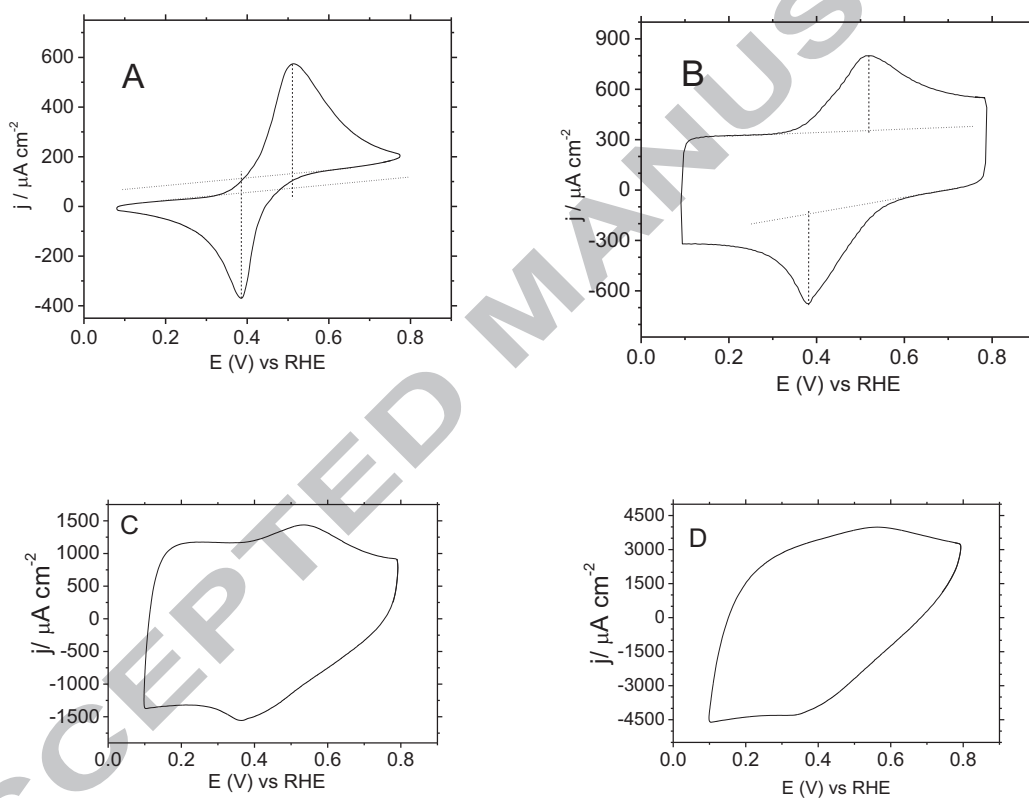

Figure 4: Steady-state cyclic voltammograms obtained in 1mM ferrocene aqueous solution for a bare GC electrode (A) and for increasing amounts (46.5, 202 and 815 μg cm^{-2}) of PEDOT-PSS deposited on GC substrates (B to D). Background electrolyte 0.5M H_2SO_4 in all cases. Scan rate 100 mV s^{-1}.

The activity of PEDOT-PSS against the same redox probe can be observed in Figures 4B to 4D. A current plateau whose shape resembles a double-layer charging current appears between 0.1 V and 0.3 V on the CV of the 46.5 μg cm^{-2} PEDOT-PSS film (Figure 4B). This featureless potential region is followed by the onset of ferrocene oxidation at 0.3 V and then by the associated anodic peak centred at 0.518 V. In the reverse scan, the faradaic counter-process appears at 0.382 V giving rise to a peak separation close to 136 mV. Figures 4C and 4D shows similar experiments performed for higher amount of deposited polymer. Current densities coming from PEDOT-PSS, below 0.3 V, increase at increasing amounts of deposited polymer. However, the redox peaks related to electron transfer from ferrocene seem progressively hindered, suggesting that PEDOT-PSS is a poor electrocatalytic material for this redox probe.

Further analysis was performed over the voltammetric results to evaluate the kinetics of the electron transfer across the polymer. The kinetic reversibility of the electrochemical reaction was evaluated from peak separation of the redox process of the cyclic voltammetry experiments by applying either the method of Nicholson [38] (see the supporting information and reference [15] for more details). In such experiments, stabilized cyclic voltammograms for bare GC electrodes and PEDOT-PSS films immersed in test solutions containing ferrocene were obtained at different scan rates ranging from 10 to 200 mV s^{-1}. The values of peak separation for a scan rate of 100 mV s^{-1} are shown in figure 5A.
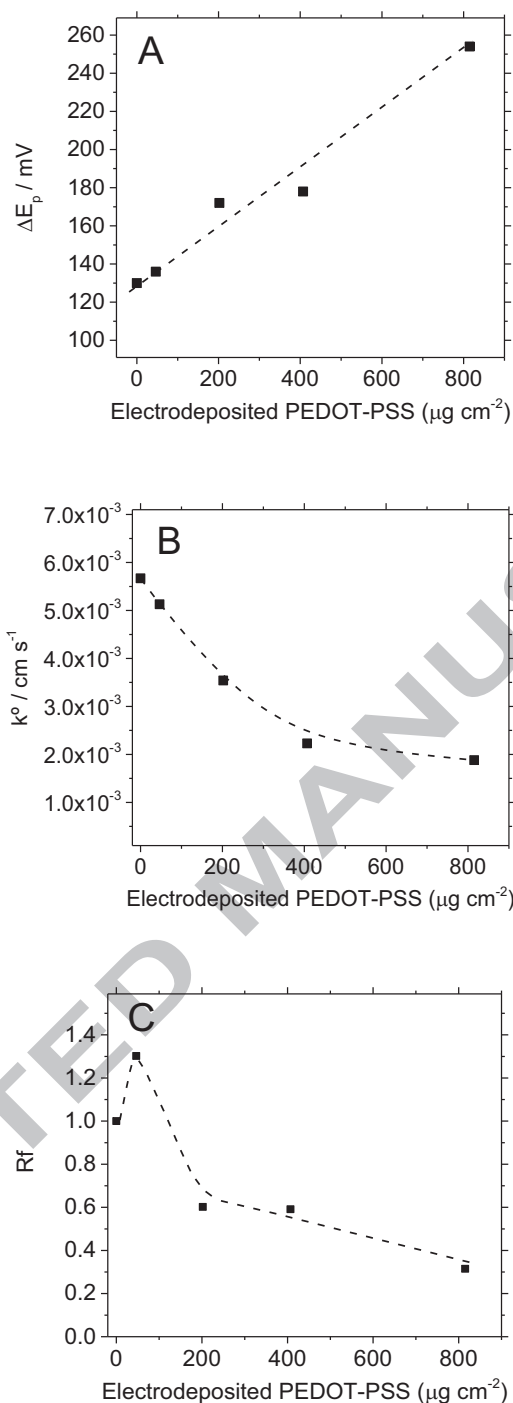
14

Figure 5: (A) Voltammetric peak separation, (B) heterogeneous rate constant for the electron transfer to ferrocene, k^o, at bare GC electrodes and at PEDOT-PSS films (C) roughness factor, R_f, obtained from the ratio between the electroactive area for the electron transfer and the surface geometric area (Data obtained from the kinetic study presented in the S.I.).

15

From the kinetic study it is derived that the standard heterogeneous rate constant for the charge transfer to ferrocene is $k^o = 5.67 \times 10^{-3}$ cm s^{-1} for bare GC electrodes, while for PEDOT-PSS films are presented in Figure 5B. The trend is that the rate of electron transfer decays at higher amounts of deposited PEDOT-PSS films up to a value close to $k^o = 2 \times 10^{-3}$ cm s^{-1}. This result confirms that unmodified PEDOT-PSS is a poor electrocatalyst to oxidize ferrocene. Another relevant parameter that can be obtained from Randles-Sevcik plots is the true active area available for the electron transfer to the redox probe (see Figure S2B). Such a parameter can be evaluated through the roughness factor of the electrode, R_f, which represents the ratio of electroactive area that transfers charge effectively to the redox probe to the geometric area [15,39]. Figure 5C shows R_f factors calculated for the reaction of interest at each electrode. As observed, an extremely thin PEDOT-PSS film shows even higher electroactive area than bare GC surfaces. However, increasing the amount of polymer results in a gradual loss of the active area up to values below a half of the geometric area.

These results can be explained in the light of FESEM and XPS characterizations performed above. On the one hand, the surface of electrodeposited polymer films appeared very smooth which implies a low roughness factor. This is probably due to the plasticizer effect induced by PSS in addition to the soft conditions used for the synthesis (potentiodynamic polymerization at moderate scan rate). On the other hand, XPS results have shown that the relative content of PSS anionic dopant, and consequently the doping level, is influenced by the mass of electrodeposited polymer. The higher the amount of deposited polymer, the lower the doping level. This trend means that films

16

with higher amount of polymer show probably less conductivity, which could disturb their electrocatalytic performance against the redox probe.

3.3. Electrochemical behaviour of ferrocene at hybrid silica PEDOT-PSS electrodes

It is known that chemically modified, porous SiO_2 matrices possess the ability of improving the kinetics of several electrochemical reactions [10,15,40]. This effect is achieved thanks to the particular environment provided by silica pores, which can rearrange electroactive molecules, change their diffusion transport properties and even stimulate favourable, or adverse, electrostatic interactions. In this section, we will try to modify the activity of PEDOT-PSS towards the oxidation of ferrocene by inserting the polymer through a three-dimensional silica matrix deposited previously on the GC surface [10].

After silica was deposited on GC, the electrode was rinsed with ultrapure water and kept humid (in hydrogel state) to be immersed in an aqueous solution containing both EDOT and PSS under experimental conditions similar to those in Figure 1. The polymer was deposited potentiodynamically until a capacitance of 14.1 mF cm^{-2} was reached. On a flat GC surface such a capacitance value corresponds to a PEDOT-PSS mass density close to 202 μg cm^{-2}. [30] However, when the polymer is grown within the silica template, those 14.1 mF cm^{-2} means that equivalent amounts of *electroactive* material have been deposited.

We should focus first on the morphology of such electrochemically deposited SiO_2 layer, which is shown in Figures 6A and 6B at different magnifications. The deposit looks homogeneous all over the surface, with randomly distributed pores

17

showing an approximate diameter of around 2 microns. The granular structure that can be distinguished in the magnified micrograph (B) comes from the aggregation of silica colloids upon deposition.
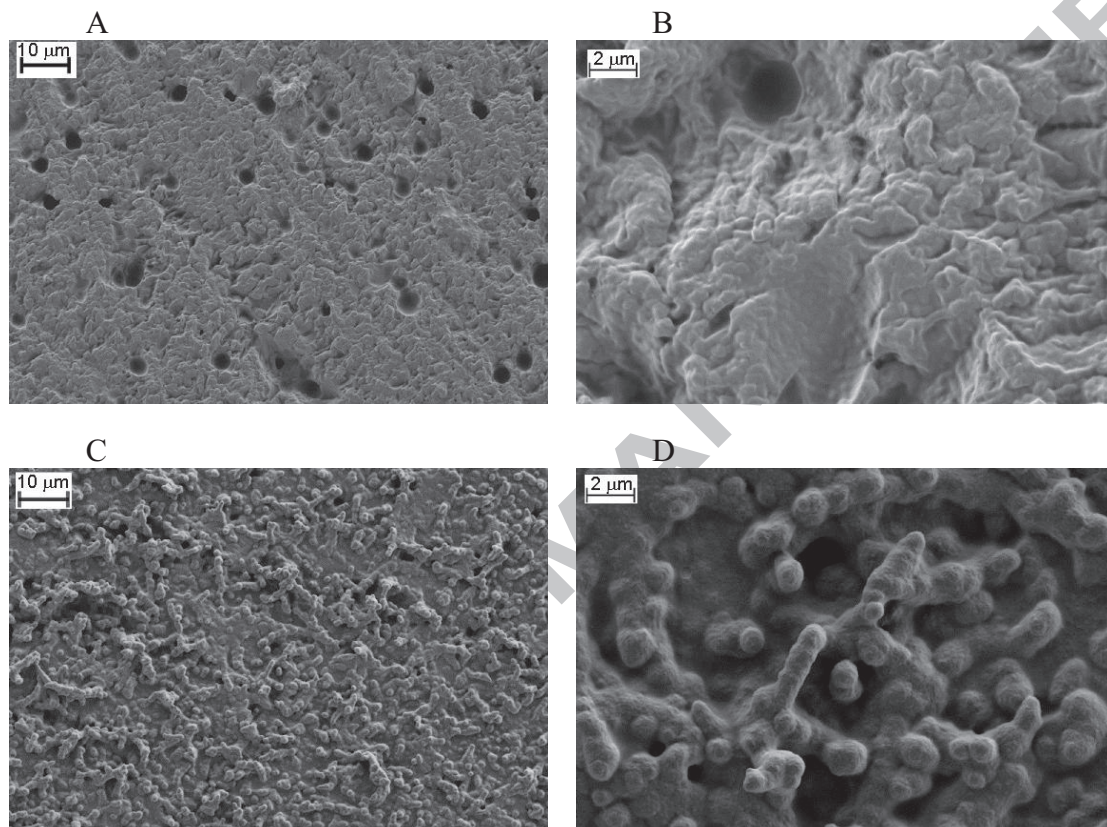

Figure 6: A and B: FESEM images of silica-modified electrodes prepared by electrodeposition. C and D: Hybrid silica-PEDOT-PSS modified electrodes.

Figures 6C and 6D were obtained after the electrochemical polymerization of EDOT through the silica pores shown in the previous images. The resulting hybrid silica-PEDOT-PSS electrode shows rounded edge, broad (near one micron) dendritic structures, which provide the modified sample with an aspect quite different to the

18

smoother, unmodified polymer films shown in Figure 2. These striking architectures are formed by PEDOT-PSS emerging from the silica material (which can be discerned as a flat surface behind the dendrites) and their particular shape is a consequence of the patterned growth of the polymer forced by the three-dimensional hollow structure of SiO_2. The hybrid material was also characterized by XPS spectroscopy and the results are shown in Figure 7.
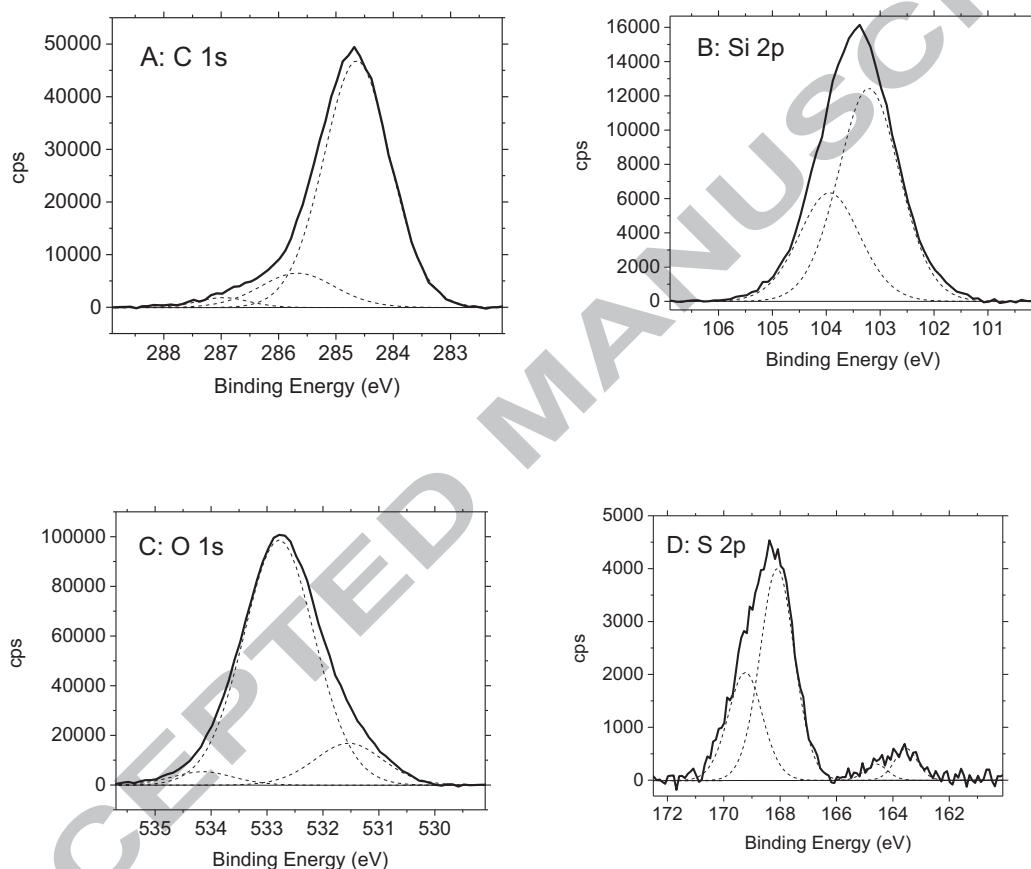

Figure 7: High-resolution XPS spectra obtained for: (A) C 1s region; (B) Si 2p region; (C) O 1s region and (D) S 2p region of hybrid silica-PEDOT-PSS film (14.1 mF cm^{-2}) deposited on a glassy carbon substrate.

19

The C1s core level spectrum shown in Figure 7A presents the three main features at 284.5, 285.5 and 286.8 eV already observed for unmodified PEDOT-PSS films in Figure 3A. They are assigned, respectively, to aromatic carbon in both PEDOT and PSS, C atoms bound to S atoms and C-O in EDOT units. Figure 7B shows the binding energy region at around 103 eV, which reveals the presence of oxidized silicon atoms on the surface, SiO_x (x>1.8) [41–43]. The presence of both C and Si signals in the outer surface (with a C/Si atomic ratio close to 2.7) supports the occurrence of an interpenetrating hybrid material. The O 1s region in Figure 7C shows three major contributions at 531.5, 532.8 and 534.2 eV. The peak at lower binding energy corresponds to the sulfonate groups of PSS [34], while the main feature at 532.8 is attributed to inorganic O bound to Si atoms of the silica matrix [44,45]. The higher binding energy peak corresponds to both, oxygen in the dioxyethylene bridge of EDOT units and the high binding energy contribution of PSS [36].

The chemical composition of a PEDOT-PSS polymer grown across the silica matrix can be investigated by exploring the S 2p region in Figure 7D. The presence of two major signals corresponding to different sulphur species allows the doping level of the polymer to be quantified, as it was done in Figure 3C. The low energy signal comes from sulphur atoms located at EDOT centres while the higher binding energy peak is attributed to sulphur in PSS. In this case, the atomic ratio of sulphur in PSS to sulphur in EDOT is 10.0. Such a large value reveals that the doping level of this polymer is significantly higher than any of the films deposited on bare GC surfaces. Therefore, it is necessary to establish whether or not a higher doping level means in practice better electrocatalytic performance to transfer charge to ferrocene.

According to such strategy, Figure 8 shows two cyclic voltammograms recorded in 1 mM ferrocene solution. The dotted line was obtained for a 202 μg cm^{-2} PEDOT-

20

PSS film deposited straight on the bare GC surface while the solid line was recorded with a silica-PEDOT-PSS hybrid material containing the same amount of electroactive polymer inserted within the SiO$_2$ pores.
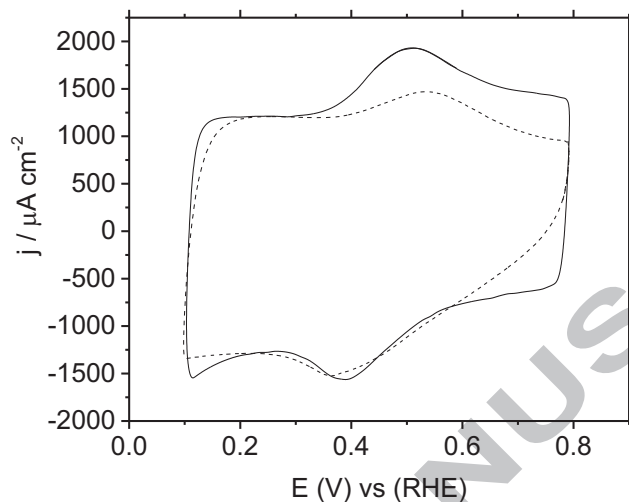

Figure 8: Steady-state cyclic voltammograms recorded in 1mM ferrocene with two different electrodes. Solid line: a hybrid material silica-PEDOT-PSS obtained by electropolymerization of EDOT on a GC previously modified with a layer of silica. Dotted line: an unmodified PEDOT-PSS film deposited on bare GC. The same amount of electroactive PEDOT-PSS was incorporated at both electrodes. Background electrolyte 0.5M H$_2$SO$_4$. Scan rate 100mV/s.

Since the amount of electroactive PEDOT-PSS sites is the same, both CVs present similar pseudocapacitive currents below 0.3 V. However, the major difference arises in the potential region for the electron transfer to the redox probe. The anodic peak associated to ferrocene oxidation appears at 0.514 V for the hybrid material. Since the faradic counter-process is centred at 0.388 V, the peak separation becomes ΔE_P= 126

21

mV. Such a value is significantly lower than those 172 mV obtained for the polymer deposited on bare GC (dotted line). According to the procedure described in the supporting information, it was determined that the standard rate constant for the charge transfer at the hybrid electrode was $k^o = 6.02 \times 10^{-3}$ cm s^{-1}. This figure means that the electron transfer rate almost doubles that measured in the absence of a silica matrix, which according to Figure 5A approaches to $k^o = 3.6 \times 10^{-3}$ cm s^{-1}. Apart from the improvement in the charge transfer kinetics, it deserves also attention the alteration of the electroactive area in PEDOT-PSS caused by the silica matrix. Making use of the Randles-Sevcik equations at different scan rates (see Figure S5) the electroactive area for ferrocene oxidation on a modified polymer gives a value close to $R_f = 2.31$, which is almost four times that obtained for a pristine PEDOT-PSS (Figure 5B).

4. Conclusions

PEDOT-PSS can be electrodeposited on bare GC surfaces from aqueous solutions containing EDOT monomer in the presence of PSS anions. After electropolymerization, XPS revealed an excess of PSS dopant for extremely thin samples and a progressive depletion of these polyelectrolyte ions as the amount of deposited polymer increases. The unmodified PEDOT-PSS material is a poor electrocatalyst toward the oxidation of ferrocene. Indeed, it has been found that the electron transfer rate decays progressively as the amount of polymer deposited increases.

The modest electrochemical performance of pristine PEDOT-PSS films can be overcome by growing the polymer through a silica matrix deposited previously on the GC surface. Contrary to the smooth surface of unmodified PEDOT-PSS films, the organic-inorganic hybrid material exhibits three-dimensional structures, as a result of

the patterned growth. The electron transfer constant for ferrocene oxidation almost doubles when the electrochemical reaction takes place on this modified polymer and, in addition, the doping level of PEDOT multiplies by a factor of three those found for films of similar electroactive mass deposited on bare GC surfaces. Such an effect is accompanied by a significant increase in the true active area available for the electron transfer to the redox probe.

5. Acknowledgments

References

[1]   M. Labib, E.H. Sargent, S.O. Kelley, Chem. Rev. 116 (2016) 9001–9090.

[2]   B.J. Sanghavi, O.S. Wolfbeis, T. Hirsch, N.S. Swami, Microchim. Acta 182 (2015) 1–41.

[3]   A. Walcarius, Anal. Bioanal. Chem. 396 (2010) 261–272.

[4]   M.M. Collinson, A.R. Howells, Anal. Chem. 72 (2000) 702 A-709 A.

[5]   R. Makote, M.M. Collinson, Chem. Mater. 10 (1998) 2440–2445.

[6]   A.R. Howells, P.J. Zambrano, M.M. Collinson, Anal. Chem. 72 (2000) 5265–5271.

[7]   D. Salinas-Torres, F. Montilla, F. Huerta, E. Morallón, Electrochim. Acta 56 (2011) 3620–3625.

[8]   A. Walcarius, Chem. Mater. 13 (2001) 3351–3372.

[9]   A. Walcarius, D. Mandler, J.A. Cox, M. Collinson, O. Lev, J. Mater. Chem. 15

(2005) 3663–3689.

[10] M. Porcel-Valenzuela, A. Salinas-Castillo, E. Morallón, F. Montilla, F.M. María Porcel-Valenzuela, Alfonso Salinas-Castillo, Emilia Morallón, Sensors Actuators B Chem. 222 (2015) 63–70.

[11] S. López-Bernabeu, A. Gamero-Quijano, F. Huerta, E. Morallón, F. Montilla, J. Electroanal. Chem. 793 (2017) 34–40.

[12] I. Gill, A. Ballesteros, Trends Biotechnol 18 (2000) 282–296.

[13] A. Salinas-Castillo, J.F. Fernandez-Sanchez, A. Segura-Carretero, A. Fernandez-Gutierrez, Anal. Chim. Acta 550 (2005) 53–60.

[14] F. Montilla, M.A. Cotarelo, E. Morallón, J. Mater. Chem. 19 (2009) 305.

[15] A. Gamero-Quijano, F. Huerta, D. Salinas-Torres, E. Morallón, F. Montilla, Electrocatalysis (2014) 33–41.

[16] S.Y. Yang, J.A. DeFranco, Y.A. Sylvester, T.J. Gobert, D.J. Macaya, R.M. Owens, G.G. Malliaras, Lab Chip 9 (2009) 704–708.

[17] D. Liu, M.M. Rahman, C. Ge, J. Kim, J.-J. Lee, New J. Chem. 41 (2017) 15458–15465.

[18] M. Mazloum-Ardakani, E. Amin-Sadrabadi, A. Khoshroo, J. Electroanal. Chem. 775 (2016) 116–120.

[19] G.X. Wang, Y. Qian, X.X. Cao, X.H. Xia, Electrochem. Commun. 20 (2012) 1–3.

[20] S. López-Bernabeu, F. Huerta, E. Morallón, F. Montilla, J. Phys. Chem. C 121 (2017) 15870–15879.

[21] J. Park, H.K. Kim, Y. Son, Sensors Actuators B Chem. 133 (2008) 244–250.

[22] P. Santhosh, K.M. Manesh, S. Uthayakumar, S. Komathi, A.I. Gopalan, K.-P. Lee, Bioelectrochemistry 75 (2009) 61–66.

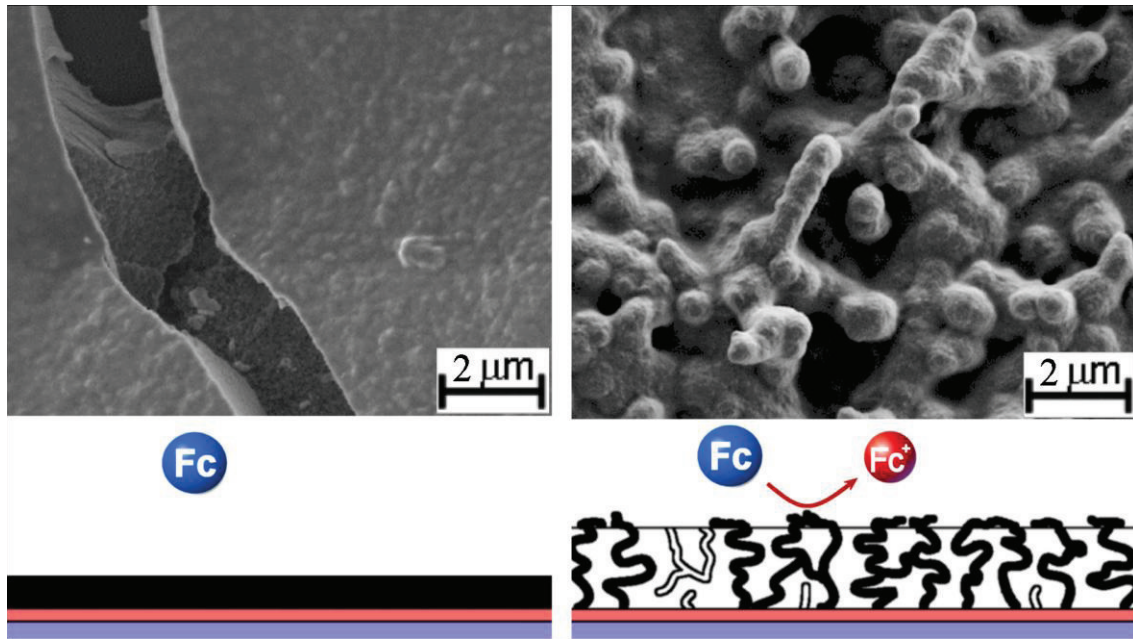[23] R.L. McCreery, Chem. Rev. 108 (2008) 2646–2687.

[24]   G. Liu, J. Liu, T. Böcking, P.K. Eggers, J.J. Gooding, Chem. Phys. 319 (2005)
        136–146.

[25]   *,† John F. Smalley, ‡ Harry O. Finklea, § Christopher E. D. Chidsey, ‖ Matthew
        R. Linford, ⊥ Stephen E. Creager, ∇ John P. Ferraris, † Keli Chalfant, ○ Thomas
        Zawodzinsk, † and Stephen W. Feldberg, M.D. Newton#, (2003).

[26]   N.J. Ronkainen, H.B. Halsall, W.R. Heineman, Chem. Soc. Rev. 39 (2010) 1747.

[27]   E.-H. Yoo, S.-Y. Lee, Sensors 10 (2010) 4558–4576.

[28]   L. Setti, A. Fraleoni-Morgera, I. Mencarelli, A. Filippini, B. Ballarin, M. Di
        Biase, Sensors Actuators B Chem. 126 (2007) 252–257.

[29]   L. Setti, A. Fraleoni-Morgera, B. Ballarin, A. Filippini, D. Frascaro, C. Piana,
        Biosens. Bioelectron. 20 (2005) 2019–2026.

[30]   J. Bobacka, A. Lewenstam, A. Ivaska, J. Electroanal. Chem. 489 (2000) 17–27.

[31]   K.C. (nee Włodarczyk), J. Karczewski, P. Jasiński, Electrochim. Acta 176 (2015)
        156–161.

[32]   V. Castagnola, C. Bayon, E. Descamps, C. Bergaud, Synth. Met. 189 (2014) 7–
        16.

[33]   A. Lachkar, A. Selmani, E. Sacher, M. Leclerc, R. Mokhliss, Synth. Met. 66
        (1994) 209–215.

[34]   S.K.. Jönsson, J. Birgerson, X. Crispin, G. Greczynski, W. Osikowicz, A.. Denier
        van der Gon, W.. Salaneck, M. Fahlman, Synth. Met. 139 (2003) 1–10.

[35]   M.M. Nasef, H. Saidi, H.M. Nor, M.A. Yarmo, J. Appl. Polym. Sci. 76 (2000)
        336–349.

[36]   G. Greczynski, T. Kugler, W.. Salaneck, Thin Solid Films 354 (1999) 129–135.

[37]   X. Crispin, S. Marciniak, J. Polym. … 41 (2003) 2561–2583.

[38]   A.J. Bard, L.R. Faulkner, Electrochemical Methods: Fundamentals and
        Applications, Wiley, New York, 1980.

[39] D. Salinas-Torres, F. Huerta, F. Montilla, E. Morallón, Electrochim. Acta 56 (2011) 2464–2470.

[40] A. Gamero-Quijano, F. Huerta, D. Salinas-Torres, E. Morallon, F. Montilla, E. Morallón, F. Montilla, Electrochim. Acta 135 (2014) 114–120.

[41] J.A. Taylor, G.M. Lancaster, A. Ignatiev, J.W. Rabalais, J. Chem. Phys. 68 (1978) 1776–1784.

[42] F.G. Bell, L. Ley, Phys. Rev. B 37 (1988) 8383–8393.

[43] X. - R Yu, H. Hantsche, Surf. Interface Anal. 20 (1993) 555–558.

[44] T. Gross, M. Ramm, H. Sonntag, W. Unger, H.M. Weijers, E.H. Adem, Surf. Interface Anal. 18 (1992) 59–64.

[45] S.S. Jedlicka, J.L. Rickus, D.Y. Zemlyanov, J. Phys. Chem. B 111 (2007) 11850–11857.

Highlights

- Electropolymerization of EDOT in aqueous PSS solution yields homogeneous films of controlled thickness.
- Electrodeposited PEDOT presents a depletion profile of PSS across the film.
- Hybrid interpenetrating silica-PEDOT improves charge transfer rate and electroactive area for ferrocene.

Graphical abstract